



1984 Ivanovo tornado outbreak: Determination of actual tornado tracks with satellite data



Alexander Chernokulsky^{a,*}, Andrey Shikhov^b

^a A.M. Obukhov Institute of Atmospheric Physics, Russian Academy of Sciences, Pyzhevsky 3, Moscow 119017, Russia

^b Department of Cartography and Geoinformatics, Perm State University, Bukireva 15, Perm 614990, Russia

ARTICLE INFO

Keywords:

Severe storm
Tornado climatology
Landsat images
Forest loss
Deep moist convection
Extreme weather event

ABSTRACT

The 1984 Ivanovo tornado outbreak is one of the most fatal tornado events in Europe with previously unspecified tornado track characteristics. In this paper, we used Landsat images to discover tornado-induced forest disturbances and restore actual characteristics of tornadoes during the outbreak. We defined boundaries of tornado-induced windthrows by visual comparison of satellite images and specified them with Normalized Difference Infrared Index. We confirmed the occurrence of eight tornadoes during the outbreak and determined their location, path width and length. Other tornadoes occurrence during the outbreak were discussed. Fujita-scale intensity of confirmed tornadoes was estimated based on the related literature corpus including previously omitted sources. In addition, information on tornado path lengths and widths was used to estimate minimal tornado intensity for those tornadoes that passed no settlements. In total, the Ivanovo outbreak includes 8–13 tornadoes with F-scale rating mean ranges from 1.8–2.5 and has adjusted Fujita length around 540 km, which makes the outbreak one of the strongest in Europe and places it within the upper quartile of U.S. outbreaks. Characteristics of certain tornadoes within the Ivanovo outbreak are exceptional for Russia. The widest tornado path during the Ivanovo outbreak is 1740 m; the longest is from 81.5–85.9 km. With the example of the Ivanovo outbreak, we showed that existing databases on historical Russian tornadoes tend to overestimate tornado path length (for very long tornadoes) and underestimate maximum tornado path width.

1. Introduction

The 1984 Ivanovo tornado outbreak is one of the most destructive tornado events in the history of Russia and among the most fatal tornadoes in Europe (Antonescu et al., 2017). The outbreak on 9 June 1984 resulted in at least 69 officially confirmed fatal victims (Vasiliev et al., 1985a, hereafter V85a); however, the exact death toll may be several times higher (Berdyshev, 2011; Finch and Bikos, 2012, hereafter FB12). Almost one thousand people were injured, and several settlements were heavily damaged or completely destroyed. One tornado during the outbreak was violent with F4 intensity on the Fujita damage scale (Fujita, 1981), which is only the second F4-tornado in the Russian history (Snitkovskiy, 1987, hereafter S87).

Despite thorough evaluation of synoptic and mesoscale aspects of the outbreak (FB12; Kapitanova, 1986; V85a), key tornado characteristics are still obscured. Particularly, a lack of systematic tornado damage survey in USSR (due to the rarity of that kind of events) resulted in relatively schematic tornado localizations and fairly approximated estimates of paths and widths of tornadoes during the outbreak. Thus,

V85a suggested the presence of four tornadoes; two of them were confirmed by eyewitnesses and two were suspected based on wind-induced forest damage analysis. S87 also indicated four tornadoes; however, they do not match with those from V85a. Using satellite images for cloud evolution, FB12 constructed paths of eight thunderstorms (TS) that produced wind damage on that day. Finally, 17 tornadoes for the outbreak were included into the European Severe Weather Database (ESWD) (Groenemeijer and Kühne, 2014, hereafter GK14). Because of the importance of the outbreak, the uncertainty on tornado's number and characteristics is needed to overcome.

The main scope of this paper is to estimate tornado characteristics for the Ivanovo outbreak using satellite-derived information on forest damage. Indeed, because the outbreak developed mostly over forested regions, it caused considerable forest loss. This kind of forest disturbances can be identified from satellite observations (Shikhov and Chernokulsky, 2018). The first attempt to utilize satellite data for assessing the aftermath of tornadoes was made by Sayn-Wittgenstein and Wightman (1975) for boreal forests of Canada. Afterward, satellite images were successfully applied to specify the characteristics of well-

* Corresponding author.

E-mail address: a.chernokulsky@ifaran.ru (A. Chernokulsky).

known remarkable tornadoes and tornado outbreaks [see e.g. (Dyer, 1988; Molthan et al., 2014; Myint et al., 2008; Yuan et al., 2002)]. Shikhov and Chernokulsky (2018) used satellite data to find previously unreported tornadoes in European Russia. They showed that Landsat information on forest loss can be used to evaluate characteristics of tornadoes with F1 intensity and higher, if they passed through forested regions.

In this paper, using Landsat satellite images, we found the actual number of tornadoes during the 1984 Ivanovo tornado outbreak, pinpointed their position, specified their path width and length with a relatively good accuracy, and compared them with the previous estimates.

2. Data and methods

To determine the exact position of tornadoes, we searched elongated windthrows that appeared in 1984 close to possible tornado locations. First of all, we focused on TS paths (from FB12) and attributed elongated windthrows that found along these paths and have the same direction to tornado-induced forest damage. Together with information on TS paths, we also verified satellite images for regions close to tornado tracks from V85a, tornado events from S87 and GK14 databases, other events from previously omitted newspapers and non-scientific literature (Androshin and Bystrova, 1984; Berdyshev, 2011; Korobeinikova, 2017; Meteoclub, 2008; Sklyarenko et al., 2009; Sklyarenko et al., 2009; Solenikov, 2006; Yakshanga Wiki, 2017).

The identification of tornado-induced forest disturbances is usually based on the analysis of satellite images obtained before and after the tornado event, preferably in the growing season [see for instance (Myint et al., 2008)]. Different change detection methods are successfully used for assessing storm- and tornado-induced forest damage; these are, for instance, univariate image differencing (Vorovencii, 2014; Wang and Xu, 2010), selective principal component analysis (Wang and Xu, 2010; Yuan et al., 2002), or vegetation indices change analysis (Vorovencii, 2014; Yuan et al., 2002). Wang and Xu (2010) showed, that the use of vegetation indices including short-wave infrared (SWIR) bands of Landsat Thematic Mapper (TM) sensor may greatly increase accuracy in detecting forest disturbances by strong winds [up to 12% compare with Normalized Difference Vegetation Index (NDVI)]. Wang et al. (2010) found that Normalized Difference Infrared Index (NDII), has higher disturbance detection accuracy than other vegetation indices (like NDVI or Enhanced Vegetation Index). NDII is calculated as:

$$NDII = (TM4 - TM5)/(TM4 + TM5),$$

where TM4 and TM5 are the reflectance in bands 4 and 5 (at 0.85 and 1.65 μm wavelengths, respectively) of Landsat TM (Hardisky et al., 1983). The TM4 reflectance correlates with plant chlorophyll content, while the TM5 reflectance has an inverse relationship with plant moisture content. Therefore, the areas with substantial decline of NDII may be reliably associated with forest cover disturbances (Toomey and Vierling, 2005).

However, the overall accuracy of automated separation of forest disturbances using spectral characteristics only does not allow to accurately distinguish windthrows from other types of disturbances, such as clear-cuttings or burned areas. For instance, the overall accuracy of automated separation of forest disturbances into windthrows and man-made cuttings does not exceed 76–77% (Baumann et al., 2014). Spectral analysis should be accompanied with evaluation of geometrical features of forest damaged areas (Shikhov and Chernokulsky, 2018). This kind of identification can be performed based on a visual analysis of geometrical characteristics of forest damaged areas by visual comparison of satellite images obtained before and after the outbreak.

Moreover, all change detection methods should be applied for images that were taken in the same phase of two growing seasons (one is before and another is after of the event). However, Landsat TM

images are available on a regular basis only from 1984, while the studied outbreak happened in the beginning of the 1984 growing season. Landsat Multi-spectral Scanner (MSS) images, which are available before 1984, have a lower spatial resolution (60 m instead of 30 m for Landsat TM) and different spectral bands (only visible and near infrared bands, without SWIR bands). Most of the obtained Landsat TM images of undisturbed forest (before the outbreak) were made in April 1984 that is earlier of the growing season beginning. Consequently, intra-seasonal NDII changes in forests may affect the results of the comparison.

Given limitations associated with the need of shape identification and absence of SWIR data for the previous growing season, we used the visual analysis of Landsat TM images as the primary step for identification tornado tracks during the studied outbreak. We used TM images, acquired from the United States (U.S.) Geological Survey (USGS) Data Center during the April and May 1984 (before the tornado outbreak), and over the summer seasons of 1984–1986 (after the tornado outbreak) (supplementary Table S1). If clouds covered the area of interest, more than one image was used. We compared the Landsat TM composite images of the TM3, TM4 and TM5 bands to find elongated forest damaged areas close to possible tornado locations (TM3 is the reflectance in band 3 at 0.71 μm wavelength).

In total, we have identified eight tornado tracks. Fig. 1 presents an example of two tornado tracks, which were identified by visual comparison of satellite images (see also supplementary Fig. S1). In addition, we have identified two amorphous forest damage areas, which could have also been caused by tornadoes or by downbursts, which may be observed during tornado outbreaks [see for instance (Forbes and Wakimoto, 1983; Peyraud, 2013)]. Lack of aerial images does not allow us to accurately discriminate the damaging mechanism of these two amorphous areas. In total, we analyzed 41 Landsat TM images and one Landsat MSS image to pinpoint tornado tracks (supplementary Table S1).

The second step was to specify discovered tornado track boundaries with NDII difference ($\Delta NDII$) for each pair of images. Firstly, the classification into four classes (forests with prevailing of coniferous, forests with predominance of deciduous, non-forested areas, clouds and clouds shadows) was performed using the Iterative Self-Organizing Data Analysis Technique Algorithm (Ball and Hall, 1965). We used the TM3, TM4 and TM5 bands as input for the classification. The unsupervised classification method was applied since the absence of ancillary data on tree species composition did not allow using this information as training samples. Therefore, we distinguished between coniferous and deciduous forests using the spectral difference in the so-called “Near-infrared plateau” (0.75–1.30 μm) (Cipar et al., 2004). Then, non-forested regions and cloudy regions covered by clouds or cloud shadows were excluded. Consequently, NDII was calculated only for the forested regions for images obtained before and after the tornadoes. $\Delta NDII$ were computed (where $\Delta NDII = NDII_{\text{before}} - NDII_{\text{after}}$).

Fig. 2 presents an example of $\Delta NDII$ for two tornado tracks (see also supplementary Figs. S2–S3). Because of intra-seasonal changes, $\Delta NDII$ varies for the 5-km zone around the track (that consists mostly of undisturbed forest) between -0.01 and -0.02 (see supplementary Table S2). Instead, $\Delta NDII$ is mostly positive for disturbed areas in the tornado track (especially for coniferous forest). To specify the boundaries of tornado tracks, we focused on pixels with values of $\Delta NDII$ that lie in the upper quartile of all pixels within the 5-km zone of the track (Table S2). Because of several peculiarities like swamped terrain (in the tornado track #4) or a long period between images [more than two years because of cloud effects (for the tornado track #6)], we had to check all areas with such high values of $\Delta NDII$ manually. This analysis allowed us to specify tornado track boundaries that were primary obtained by composite images visual comparison.

Boundaries of identified tornado tracks were used to determine tornado characteristics such as tornado path length L_{tp} , mean and maximum tornado path width (WM_{tp} and WX_{tp} , respectively), and

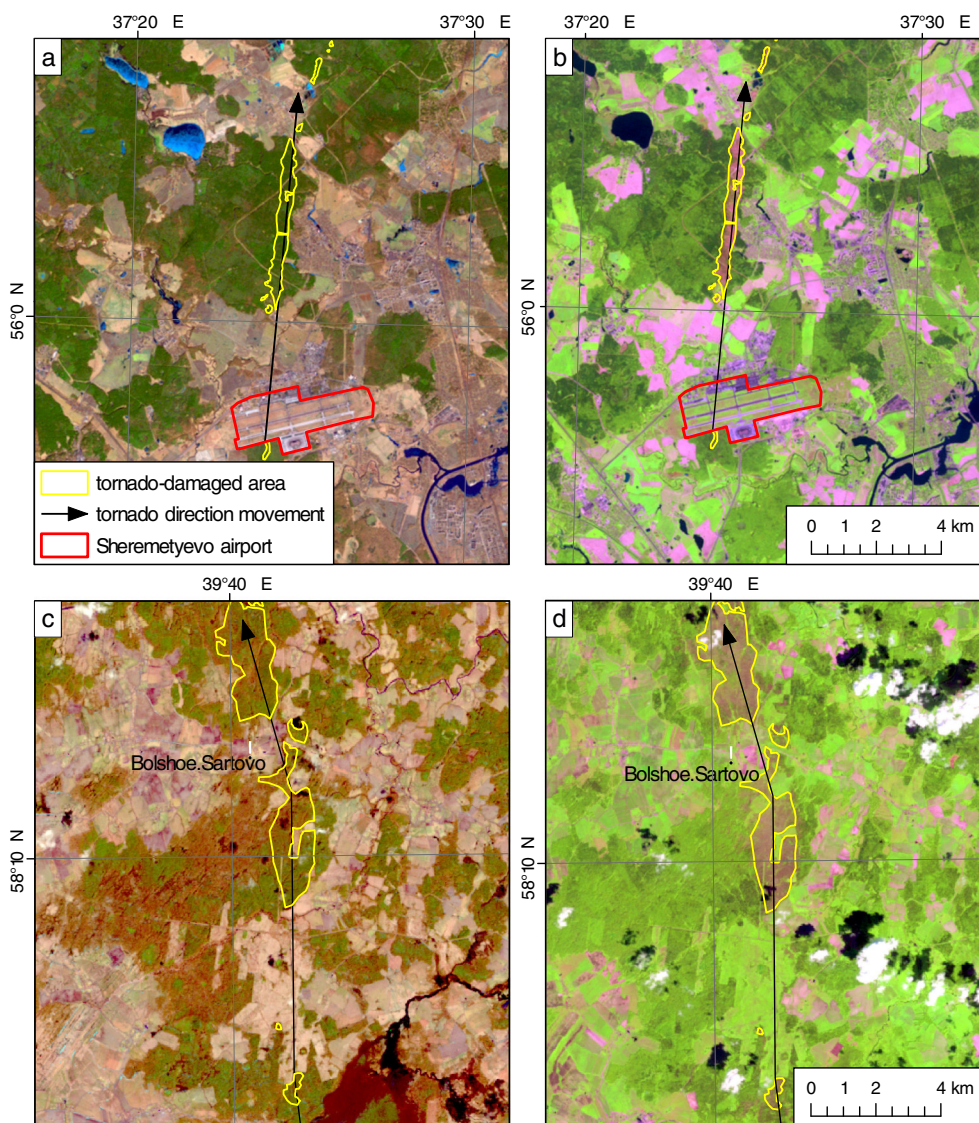


Fig. 1. Composite Landsat TM images (combination of the TM3, TM4 and TM5 bands), acquired before (a, c) and after (b, d) the Ivanovo outbreak, for the tornado tracks #1 (a, b) and #5 (c, d). Tornado-damaged area is outlined with the yellow contour; general direction of tornado movement is shown with the black arrow. Sheremetyevo airport and Bolshoe Sartovo village are depicted. (For interpretation of the references to colour in this figure legend, the reader is referred to the web version of this article.)

forest damaged area (A_{tp}). L_{tp} and WM_{tp} were determined following the procedure from Shikhov and Chernokulsky (2018), L_{tp} was defined as a length of the central line drawn through a damaged area (between the outermost points of the most distant areas of forest disturbances) and calculated using ArcGIS. WM_{tp} was calculated by averaging transects that drawn every 200 m perpendicular to the observed tornado path (without accounting for undisturbed forested and treeless areas). The 200 m step was found to be optimal in terms of accuracy and effectiveness for computing WM_{tp} (Shikhov and Chernokulsky, 2018). WX_{tp} was measured manually by Landsat images. A_{tp} was calculated in ArcGIS as the sum of all identified forest damaged forested areas that attributed to the tornado.

We can estimate tornado characteristics with limited accuracy. In particular, Shikhov and Chernokulsky (2018) showed that Landsat-based estimates of WM_{tp} and WX_{tp} have an accuracy of 10%. L_{tp} tends to be underestimated when a tornado starts or terminates outside out of forest boundaries (or becomes too weak to make a damage). Therefore, we provide two estimates of L_{tp} : minimal that equals to the distance between the outermost points of the most distant areas of forest disturbances within one track, and maximal that includes the length of preceding (following) unforestated terrain from previous (to the next)

undisturbed forest (see Table S3 for information about terrain feature of the beginning and ending of the tornado tracks).

All found tornado tracks have gaps. These gaps come from forest discontinuity, tornado intensity fluctuation or short-term lifting of the tornado from a surface (so called “skipping tornadoes”) (Doswell III and Burgess, 1988). In a skipping, but continuous tornado, 5–10 miles (8–16 km) are accepted as a maximum size for gaps (Doswell III and Burgess, 1988). We used an 8-km threshold for the gap that fully covered by forest to separate one skipping tornado from two successive tornadoes (see Table S3 for details on tornado gap characteristics).

We addressed part of analysis to evaluation of Fujita-scale tornado intensity (FI). In addition to the previously published estimates (GK14, S87), we provided new estimates that based on previously omitted damage reports in media. Moreover, since some tornadoes passed through uninhabited forested areas, we evaluated minimal FI given information on L_{tp} and WX_{tp} . We used Weibull distribution parameters that tied L_{tp} and WX_{tp} with FI (Brooks, 2004) to evaluate the probability of a minimal tornado FI following the approach proposed by Shikhov and Chernokulsky (2018). For each tornado we determined the most reliable estimate of FI among all estimates for the particular tornado. To keep the consistency with the previous estimates, we did not evaluate

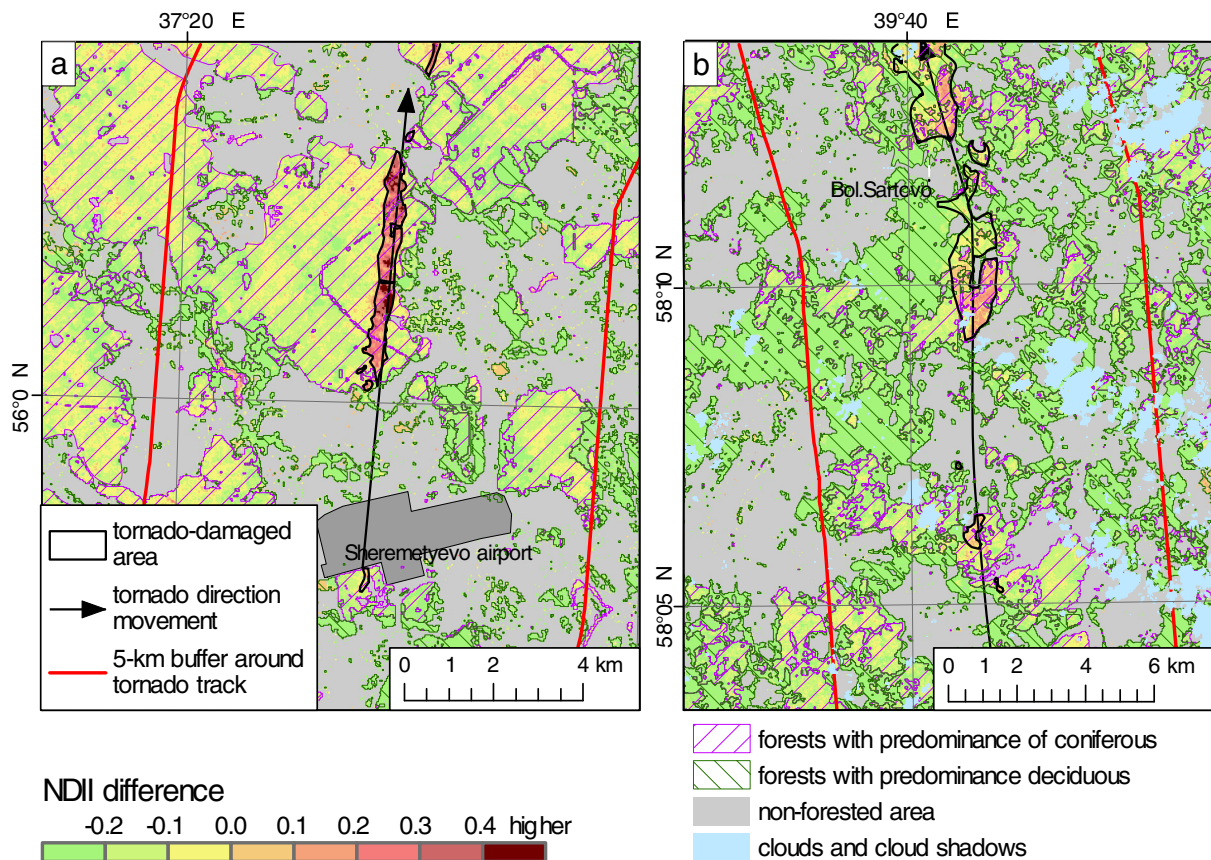


Fig. 2. Normalized Difference Infrared Index (NDII) difference calculated by Landsat TM images obtained before and after the Ivanovo tornado outbreak, for the tornado tracks #1 (a) and #5 (b). Tornado-damaged area is outlined with the black contour; general direction of tornado movement is shown with the black arrow. 5-km zone around the track is shown with the red boundaries. Non-forested areas are shown with grey shading. Clouds and cloud shadows are shown with blue shading. Purple right-inclined lines stand for regions with the predominance of coniferous forests; dark green left-inclined lines stand for regions with the predominance of deciduous forests. (For interpretation of the references to colour in this figure legend, the reader is referred to the web version of this article.)

enhanced Fujita (EF) (McDonald and Mehta, 2006) scale rating of the outbreak tornadoes. While EF-scale is widely used in U.S., proper usage of EF-scale in Russia demands first to propose and validate appropriate damage indicators and degrees of damage that would take into account Russian construction practices [for instance, as performed in Japan (Okada et al., 2015)].

For each tornado, coordinates of the start, the center, and the end of its track are provided (Supplementary Table S4). The supplementary shp-file contains the polygons of forest damaged areas and detailed information on tracks (see Supplementary mapping material).

3. Results and discussion

The synoptic and mesoscale aspects of the Ivanovo tornado outbreak were thoroughly evaluated in previous studies (FB12; Kapitanova, 1986; V85a). They clearly showed that the atmospheric conditions were favorable for deep moist convection (DMC) development. All so-called “ingredients” that are necessary for DMC (Doswell III and Evans, 2003; Johns and Doswell III, 1992; Taszarek et al., 2017) were in place in the center of the European part of Russia on 9 June 1984. First, an advection of moist maritime air masses from the Black sea within fast-moving low-troposphere cyclone and local evapotranspiration determined high boundary layer moisture content with amount of precipitable water up to 30 mm (FB12). Second, the advection of moist air from south and southeast in boundary layer was accompanied with a strong southwesterly upper-level jet stream that brought dry air to the middle troposphere (V85a, FB12). This caused a particular high instability with convective available potential energy (CAPE) >

2300 J kg⁻¹ and high values of wind shear (the 0–6 km deep layer shear > 30 m s⁻¹, the 0–3 km storm relative helicity > 300 m² s⁻²) (FB12). Finally, strong air convergence in the lower troposphere resulted in an exceptional strong lifting in the middle troposphere (V85a). Magnitudes of updraft and kinetic energy generation within the cyclone of 9 June 1984 were comparable to those in well-developed tropical hurricanes (Kapitanova, 1986).

A set of indicated conditions led to formation of several TSs with the cloud top height penetrating the tropopause (up to 14 km) (V85a). Associated weather radar echoes presented “an extremely high radar reflectivity” (V85a); although, the radar data itself are not preserved (A. Vasiliev, personal communication). The passing of these TSs was accompanied by a complex of severe weather events (tornadoes, wind gusts, hail, heavy showers) (V85a). Paths of TSs were pinpointed by FB12 based on Meteosat-2 imagery for cloud evolution. However, the exact locations of tornadoes were still unclear.

Fig. 3 presents the results of the tornado track identification during the 1984 Ivanovo tornado outbreak. Additionally, previous estimates of tornado positions (V85a; S87, GK14) and TS paths (FB12) are depicted. Table A1 (see the Appendix) summarizes information on characteristics of verified and possible tornadoes of the day.

The most western TS (storm “A” according to FB12) yielded three tornadoes, more than other thunderstorms that day. The first tornado (#1) is well known and was captured by many eyewitnesses; it passed through the Sheremetyevo airport, damaged air-shed, three aircrafts, and a forested area located to the north of the airport (Sheremetyevo 50th, 2009). We found that the tornado strengthened after crossing the airport, increasing its path width (its actual WX_{tp} is five times larger

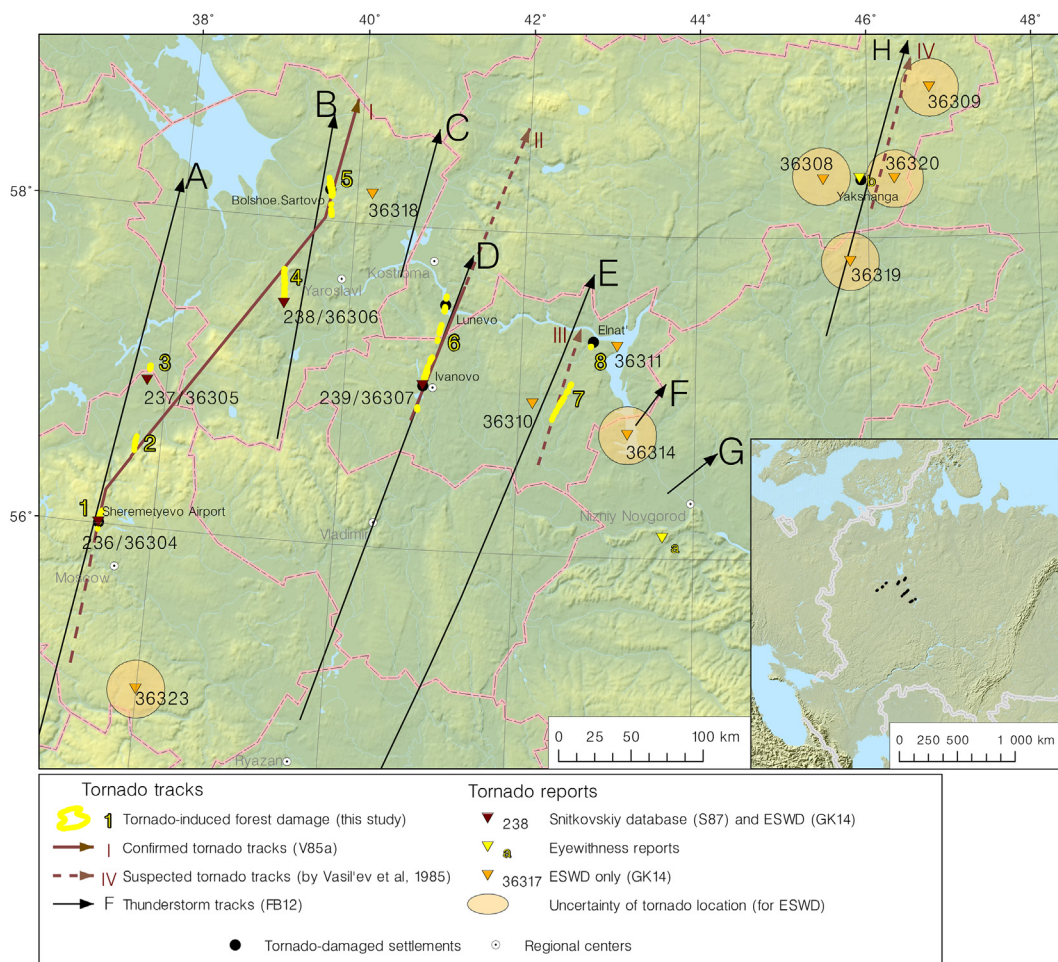


Fig. 3. Tornado and storm tracks on June 9, 1984 from different data. Yellow contours show tornado-induced treefalls obtained in this study from Landsat satellite data (with the corresponding order numbers). Dark brown triangles stand for tornadoes from Snitkovskiy (1987) and ESWD (Groenemeijer and Kühne, 2014) databases (with the corresponding identical numbers in that databases), orange triangles stand for tornadoes from ESWD only (with the corresponding identical numbers and location uncertainty). Yellow triangles and lowercase letters show tornado events obtained from eyewitness reports. Brown arrows show tornado paths that obtained by V85a (solid lines show tornado tracks, that had been confirmed at that time and dashed lines show suspected tornado tracks) (with the corresponding Latin letter), black arrows show mesoscale convective system tracks (from Finch and Bikos, 2012) (with the corresponding capital letters). Tornado-damaged settlements are shown with black filled circles. The inset displays a general map of the European part of Russia with the localization of the confirmed outbreak tornadoes. (For interpretation of the references to colour in this figure legend, the reader is referred to the web version of this article.)

than was mentioned previously), and likely its intensity (Table A1). We discovered the second tornado track in a forest 60 km north of Moscow. This tornado is previously unreported, since it missed settlements and had no eyewitnesses. The third tornado passed near Volosovo village. S87 included it into his database with unspecified path and length. Intensity was estimated as F0 since the tornado did not affect any construction. However, comparatively large L_{tp} and WX_{tp} (see Table A1) likely point to a higher intensity ($\geq F2$).

TS “B” yielded two tornadoes in the Yaroslavl region. Related areas of destruction were erroneously attributed by S87 to the one long tornado track with 100 km path length. We show that L_{tp} should be four times less for both tornadoes (Table A1). On the contrary, tornado path width was previously underestimated. Thus, for the tornado #4, WX_{tp} and WM_{tp} from satellite data are comparable for those from S87; however, the tornado #5 has three times larger WX_{tp} than assumed before. In fact, it has the largest WX_{tp} among all tornadoes during that day (and hence the largest A_{tp}) (Table A1). This tornado completely destroyed the village Maloe Sartovo (Solenikov, 2006). Given tornado damage description, we defined its intensity as F3. Intensity of the tornado #4 was estimated by S87 as F3; however, there is no clear indication, how exactly this rating was done. Our findings show that tornado formed 6.5 km northeast from Golubkovo village mentioned by S87 (FB12 drew wrong Golubkovo on their map on Fig.16). Sklyarenko

et al. (2009) pointed ending of this tornado in peatlands near Varegovo village, that is supported by Landsat images analysis. Consequently, the tornado #4 did not pass any settlements. Since S87 assumed a single track for the tornadoes #4 and #5, it is likely that his estimate was based on damages in Bolshoe and Maloe Sartovo villages and should belong to the tornado #5.

The most violent and devastating tornado (#6) was associated with TS “D”. The tornado formed to the south of the city of Ivanovo, hit Ivanovo suburban, and destroyed Lunevo campsite. Despite well-documented tornado impact (Alimov et al., 1984; Berdyshev, 2011; FB12; Lyakhov, 1986; Sklyarenko et al., 2009; V85a; Vasiliev et al., 1985b), authors disagree on its intensity rating. In particular, V85a and S87 estimated the intensity at F4 rating; while, GK14 assumed it had F5 rating. GK14 made their assumption (T. Kühne, personal communication) considering mainly the fact, that “tornado moved 50 ton water tank for 200 m” (V85a), that is in concordance with the F5 damage specification “automobile-sized missiles fly through the air in excess of 100 m” (Fujita, 1981). However, the watertank located on a water-tower in a 20–30 m height. The elevated position presumably helped it to fly a 200 m distance. V85a mentioned, that concrete and large brick houses were not destroyed, but had their roofs torn off. We therefore suppose that F4 rating is a more correct estimate of the tornado #6 intensity. Additionally, we found that the tornado weakened or lifted

between Ivanovo and Lunevo where 7.5 km of undisturbed forest were preserved along the tornado track (for more details see Supplementary materials, Table S3). We confirmed an assumption of FB12, who speculated that the tornado path length is overestimated. In particular, we found that the tornado ceased in 2.5 km after the Volga river crossing. As a result, the actual L_{tp} is almost twice less than presented by V85a and S87 (Table A1); nevertheless, the tornado #6 track is the longest during the outbreak.

TS “E” resulted in two tornadoes near Lukh and Yurievets towns. V85a mentioned forest disturbances in that area (“suspected tornado track III”); however, tornado characteristics were previously unspecified. The tornado #7 had no impact on settlements since it passed through fields of forested area. On the contrary, the tornado #8 destroyed dozens houses in Elnat’ village (Androshin and Bystrova, 1984) and likely had F3 intensity. Estimate of L_{tp} of this tornado is uncertain since it damaged only one section of forest and then hit Elnat’. We supposed that its L_{tp} is between 4.2 km and 21.7 km (Table A1).

In addition to tornado-induced elongated forest losses areas associated with the tornadoes #1–8, we found amorphous forest disturbances along TS “H” near Yakshanga village and 35 km south-east from Sharya town. V85a highlighted these disturbances as induced by tornado or squall (for instance, strong gust front of downburst). In chronicles of Yakshanga (Yakshanga Wiki, 2017), the word “tornado” (*smerch*) was mentioned (the event “b”). It tore away two roofs from houses in the northern part of the village. We can speculate with medium degree of certainty about the presence of a tornado in this region; however, this tornado can not be confirmed by satellite data on forest loss.

No forest disturbances were found with Landsat images for other possible tornado locations (Table A1). This may come from relatively low forestation of studied area, for instance, near Suna settlement (the event “c”) where strong wind [“tornado” according to Korobeinikova (2017)] damaged farms and houses and broke trees. It is mentioned, that a tree-top from a broken poplar was deeply stick into the ground at an acute angle, which may indicate the presence of the tornado. In addition, the absence of satellite-detected forest loss may be associated with too narrow area of damaged forest (comparative to the 30 m Landsat spatial resolution). Thus, we failed to reveal forest losses near Shumilovo village (the event “a”) despite the thorough description of 50 m width strips of tree damage in this region (Meteoclub, 2008). Strips of tree damage near Liubim and Sormovo that mentioned by V85a (without details) are also missed in Landsat images.

Other events and their characteristics are less certain. Particularly, the time of events in the Nizhniy Novgorod region (Table A1) is dubious. On the one hand, the events might have had a tornadic nature and formed within TS ‘F’ and ‘G’ around 11:00 UTC. On the other hand, according to V85a they might have been squalls (gust fronts of downbursts), which hit the Nizhniy Novgorod region around 14:00 UTC. V85a pointed out, that squalls with wind speed up to 30–40 m s⁻¹ were observed in the Moscow, Ryazan, Nizhniy Novgorod and Saratov regions, and in the republics of Mordovia and Chuvashia in 1–4 h after the tornadoes in Yaroslavl and Ivanovo regions. These squalls erroneously attributed to tornadoes in ESWD with unspecified locations (T. Kühne, personal communication).

Integral characteristics of the outbreak make it remarkable for Europe. In total, the Ivanovo outbreak includes from 8 to 13 tornadoes with the mean F-scale rating from 2.5 (in case of eight fully verified tornadoes) to 1.8 (in case of 13 tornadoes) (Table 1). This makes the outbreak one of the most intense among all European outbreaks and unprecedented for Russia. Particularly, it is the strongest among outbreaks with > 5 tornadoes. Moreover, only 20% of eastern U.S. outbreaks have adjusted Fujita length (AFL, see the caption of Table 1 for more details) > 540 km (335 miles) long (Fuhrmann et al., 2014). Consequently, the Ivanovo outbreak is among the strongest outbreaks in Europe and within the upper quartile of the U.S. outbreaks.

Characteristics of certain tornadoes within the outbreak are unusual

Table 1

Characteristics of the Ivanovo outbreak and its ranking among 36 European tornado outbreaks from 1900 to 2014 [from Tijssen (2015)] and 846 eastern U.S. tornado outbreaks from 1973 to 2010 [from Fuhrmann et al. (2014)]. Three cases with different degree of certainty are considered. The most reliable estimates of tornado intensity are used (see Table 1). For two tornadoes with low degree of certainty F0, intensity is assumed. Fujita length is a sum of multiplication of the tornado F-scale rating and L_{tp} for all tornadoes within the outbreak (as proposed by Fuhrmann et al. (2014)). Fujita length is calculated only for the first case (since L_{tp} is known only for the tornadoes with high degree of certainty), minimal estimate of L_{tp} is used. Adjusted Fujita length is calculated with the use of mean adjusted F-rating (from Table 1 from (Fuhrmann et al., 2014)) instead of F-rating.

	Degree of certainty of tornado events		
	High only	High and medium	High, medium and low
<i>Characteristics</i>			
Number of tornadoes	8	11	13
Mean F-intensity	2.5	2.2	1.8
Fujita length, km (mi)	598.3 (371.8)	–	–
Adjusted Fujita length, km (mi)	537.6 (334.1)		
<i>Ranking among 36 European tornado outbreaks, 1900–2014 (fromTijssen, 2015)</i>			
Number of tornadoes within outbreak	9–13	7–8	4–5
Sum of F-intensity	2	2	2
Mean F-intensity	9	14	16–17
Mean F-intensity for 26 outbreaks with > 3 tornadoes within an outbreak	2	4	6–7
Mean F-intensity for 20 outbreaks with > 5 tornadoes within an outbreak	1	2	3
<i>Ranking among 846 eastern U.S. tornado outbreaks, 1973–2010 (fromFuhrmann et al., 2014)</i>			
Adjusted Fujita length	~150–160	–	–

for Russia. Among 110 tornadoes in forested regions of western Russia, which occurred in the 21st century (Shikhov and Chernokulsky, 2018), only one tornado has $L_{tp} > 80$ km, and only two tornadoes have $WX_{tp} > 1500$ m. Fortunately, they missed settlements and had impact only on forest cover.

Our analysis allows estimating damage of the Ivanovo outbreak to the Russian forestry fund. We estimated sum of A_{tp} (ΣA_{tp}) during the outbreak around 36.5 km². Rozhkov and Kozak (1989) mentioned that the total area of forest disturbances during the severe weather events of 9 June equals to 110 km², which is three times larger than our estimates. However, any details like localizations of these disturbances or their causes (tornadoes or squalls) had been omitted. Because of coarse Landsat resolution (30 m) we may miss some narrow tornado-induced disturbances with apparently small area. Nevertheless, it is more likely, that the difference comes from the Russian foresters practice to overestimate damaged forest areas. Foresters consider scattered disturbances (for instance, when 15–30% of forest are damaged) as all over disturbances (with 100% damage area) for the purpose of sanitation cutting. Therefore, we assume that 2/3 of forest damaged area mentioned in Rozhkov and Kozak (1989) (around 73 km²) is likely squall-induced and associated with scattered disturbances. That kind of disturbances was not detected by our method of imagery visual comparison. The estimate of ΣA_{tp} obtained in this study (36.5 km²) stands only for area with total canopy removal. This area is sufficient compared with area of other tornado-induced forest disturbances. In particular, Shikhov and Chernokulsky (2018) showed that sum of A_{tp} for 110 tornadoes in forested regions of northeast Europe for 2000–2014 is 172 km², which is only 5 times higher than for eight tornadoes during the Ivanovo outbreak. However, ΣA_{tp} is negligible compared with windstorm- or fire-induced forest loss (Shikhov and Chernokulsky, 2018).

The outbreak resulted in various loss to coniferous and deciduous forests. In particular, out of 29.6 km² (that can be attributed to the specific forest type), 18.3 km² and 11.3 km² stand for damages in coniferous and deciduous forests respectively. We calculated WM_{tp} and WX_{tp} separately for coniferous and deciduous parts of each track (the supplementary Table S5) and found that WX_{tp} depends mostly on species composition in the area of tornado passing, while WM_{tp} is larger for coniferous parts for all tracks (even for the tracks #4–6 that passed through forest where deciduous dominate). This finding is in concordance with previous studies. Specifically, [Szwagrzyk et al. \(2017\)](#) showed, that the forest species composition has a significant influence on the wind-induced tree mortality. [Lassig and Mochalov \(2000\)](#) studied wind-induced forest damage in the Ural region of Russia and found that spruce and fir forests are more vulnerable to strong winds than other forests. But they also showed that forest stands age is important as well (older trees are more vulnerable). Lack of ancillary data on forest characteristics allows us to make only qualitative conclusion on greater influence of the outbreak on coniferous woods.

We showed, that previous estimates of tornado characteristics are biased. On the one hand, [S87](#) tends to overestimate tornado path length because of erroneously combining different short tornado tracks into a longer one. On the other hand, the maximum tornado paths were previously underestimated since it occurred outside of settlements (in forest). We found the longest (widest) tornado path of that day is 81.5–85.9 km (1740 m) compared with 160 km (800 m) from [S87](#). The [S87](#) database was mainly collected from eyewitnesses reports and accompanied with thorough ground surveys in very rare cases. Thus, we speculate that estimates of other tornadoes in [S87](#) database can be also biased especially for tornadoes that passed through forest regions.

Our method is imperfect as well. Tornado path width can be estimated with limited accuracy (around 10%). Tornado path length estimates are circumscribed by forest coverage; therefore, we provided two estimates of L_{tp} . Another limitation of our method is a chance to miss weak tornadoes that have no impact on forest or cause very narrow disturbance areas with width comparable or less than Landsat resolution (< 50 m) ([Shikhov and Chernokulsky, 2018](#)). Furthermore, we may miss short-lived tornadoes that developed over non-forested unpopulated areas. As a result, the actual number of tornadoes during the outbreak may be higher than that obtained in this study.

4. Conclusion

The 1984 Ivanovo tornado outbreak is one of the most remarkable tornado events in Russian history with previously unspecified tornado track characteristics. Here, we restored the exact position of eight tornado tracks during the outbreak by discriminating forest disturbances

area from Landsat satellite images. We visually compared Landsat images before and after the event to pinpoint tornado tracks and used Normalized Difference Infrared Index to specify tornado track boundaries. We used previously omitted damage reports in media and information on tornado path length and width to estimate Fujita intensity of tornadoes.

We specified tornado characteristics such as tornado path length, maximum and mean width, Fujita-scale intensity. From eight fully verified tornadoes, one had F4, three had F3, and four had as a minimum F2 intensity. We ranked the certainty of other possible tornadoes that were mentioned in the previous studies and/or in media. These events left no clear impact on forest and can not be recognized from Landsat data. In addition to eight confirmed tornadoes, we highlighted three events that likely were tornadoes (with F1–F2 intensity), two events that may be both tornadoes and squalls (gust fronts of downbursts), and six events that were erroneously included into the tornado section of ESWD. Considering new findings on the actual number and characteristics of tornadoes, the outbreak can be interpreted as the one of the strongest in Europe from 1900 (the strongest among outbreaks with > 5 tornadoes) and unique for Russia.

Obtained estimates of tornado tracks during the Ivanovo outbreak may be used for improving tornado databases (e.g. ESWD). In particular, we showed previous estimates of tornado characteristics are biased. [S87](#) database tends to overestimate tornado path length (for very long tornadoes) and underestimate maximum tornado path width. Therefore, these data should be treated given these shortcomings. In addition, the revealed tornado tracks may be used for validating results of mesoscale model simulations of the outbreak. Such simulations are worth to perform in the manner of recent studies on European tornadoes ([Matsangouras et al., 2014](#); [Novitskii et al., 2016](#); [Taszarek et al., 2016](#)) in order to improve our understanding of the processes that stands behind these events. It is especially important in the light of projected increase of tornado formation risk over northern midlatitudes under climate change ([Brooks, 2013](#); [Chernokulsky et al., 2017](#); [Kurgansky et al., 2013](#); [Půček et al., 2017](#)).

Acknowledgements

We thank two anonymous reviewers for valuable comments, and Igor Azhigov for the help with satellite images proceeding. This work was supported by the Russian Science Foundation (project no. 14-17-00806) using the results obtained within the Russian Foundation for Basic Research (projects 16-05-00245, 17-05-00561, 17-05-00695) and the RAS Program 51.

Appendix A

Table A1

Characteristics of confirmed and plausible tornadoes and thunderstorms on 9 June 1984 obtained from different data sources. For the tornado #8, L_{tp} in brackets takes into account path to Elnat' village. For the tornado #4, the 0–6 km deep layer shear (DLS, $m s^{-1}$) and the storm relative helicity for the 0–3 km layer (SRH, $m^2 s^{-2}$) are shown in addition to surface-based convective available potential energy (SBCAPE) (from FB12). Degree of certainty that tornado happened: H – high, M – medium, L – low, VL – very low. The most reliable estimates of tornado intensity are shown with the bold font.

Region, districts and place	Tornado tracks from forest disturbances					# of tornadoes (V85a)	Thunderstorm characteristics and indices (FB12)			Tornado characteristics (S87)
	#	L_{tp} , km Maximum potential length, km	WM _{tp} and WX _{tp} , m	A_{tp} , ha	Estimated FI		#	Storm motion velocity ($m s^{-1}$)	SBCAPE ($J kg^{-1}$)	
Moscow region, Solnechnogorsk and Dmitrov districts, near Sheremetyevo airport	1	13.5 13.5	267 530	198	≥ 2	I	A	20–22	~1000	227
Moscow region, Dmitrov district, near Pavlovichi village	2	11.4 13.1	187 430	123	≥ 2					–
Tver' region, Kalyazin district, near Volosovo village	3	10.9 15.0	444 690	211	≥ 2					228
Yaroslavl' region, Borissoglebsk and Bolsheselsk districts, near Golubkovo and Varegovo villages	4	27.5 46.0	335 720	684	≥ 2		B	20–22	1500–2000	229
Yaroslavl' region, Danilov district, Bolshoe Sartovo village	5	26.3 27.1	634 1740	1161	≥ 3					–
Ivanovo and Kostroma regions, Ivanovo and Furmanovo districts, Ivanovo city, Lunevo village	6	81.5 85.9	423 1130	972	≥ 3	II	D	26	2329 (DLS = 31; SRH = 307)	230
Ivanovo region, Likh district, 12 km from Likh city	7	28.5 32.0	246 600	265	≥ 2	III	E	25	≥ 2000	–
Ivanovo region, Yurievets district, 17 km from Yurievets city, Elnat village	8	0.9 (4.2) 21.7	345 410	30	≥ 2					–
Nizhniy Novgorod region, Nizhniy Novgorod district, near Shumilovo	–	–	–	–	–	–	G	–	–	–
Kostroma region, Ponazyrevo district, Yakshanga	–	–	–	–	–	IV	H	–	> 2000	–
Kirov region, Suna district, Kokui and Suna villages	–	–	–	–	–	–	–	–	–	–
Yaroslavl' region, Liubim district	–	–	–	–	–	–	C	–	–	–
Nizhniy Novgorod region, Nizhniy Novgorod district, near Sormovo	–	–	–	–	–	–	G	–	–	–
Nizhniy Novgorod region, Chkalovsk	–	–	–	–	–	–	F	–	–	–
Chuvashia republic, Alatyir district	–	–	–	–	–	–	–	–	–	–

Region, districts and place	Tornado characteristics (S87)		ESWD (GK14)		News, media, etc.	Time of the event (start, UTC)	Peculiarities (including damage description)	Degree of certainty
	length, km	Average and maximum width, m	FI	ESWD ID				
Chuvashia republic, Kanash district	-	-	-	-	-	-	-	-
Saratov region, no precise location	-	-	-	-	-	-	-	-
Moscow and Ryazan regions, no precise location	-	-	-	-	-	-	-	-
Mordovia republic, no precise location	-	-	-	-	-	-	-	-
Moscow region, Dmitrov district, near Pavlovichi village	10	75	1	36304	1	09:09	Air-shed and three aircrafts were damaged in the Sheremetyevo airport (Sheremetyevo 50th, 2009; V885a). The tornado damage track was found with Landsat images.	H
Tver' region, Kalyazin district, near Volosovo village	-	-	-	-	-	~10:00	No damage to settlements. The tornado damage track was found with Landsat images.	H
Yaroslavl' region, Borisoglebsk and Bolsheselsk districts, near Golubkovo and Varegovo villages	100	450 600	3	36306	3	~11:00	No damage to settlements. The tornado damage track was found with Landsat images.	H
Yaroslavl' region, Danilov district, Bolshoe Sartovo village	-	-	-	36318	-	~11:40	All houses in Maloe Sartovo villages were destroyed completely; houses in Bolshoe Sartovo were uprooted. A bus was heavily damaged, around 10 people died (Solenikov, 2006). Hailstones with a 15 cm diameter and a 1 kg weight were observed (Lyakhov, 1986, Vasiliev et al., 1985b) that is close to the world record (FB12). The tornado damage track was found with Landsat images.	H
Ivanovo and Kostroma regions, Ivanovo and Furmanovo districts, Ivanovo city, Lunevo village	160	550 800	4	36307	5	12:05	Concrete houses in Ivanovo were damaged (roofs were torn away, glasses were broken out), trees posts and power lines supports were broken/ uprooted, wooded houses in surrounding villages near Ivanovo and in Lunevo were destroyed, heavy railroad cars were overturned; cars, buses, trolleys, a crane (with 350 ton weight) and other objects in Ivanovo were lifted up, flipped and dumped onto their sides; graveyard in Balino was destroyed; asphalt was pulled up and scattered on a highway near Ivanovo; a 50 ton watertank was moved for 200 m; people injured (around 1 thousand) and died (dozens or hundreds); up to 5 suction vortices made 50-m width strips of forest damage around the main tornado path (Alimov, 1984; Bertdyshev, 2011; Lyakhov, 1986; Sklyarenko et al., 2009; V85). The tornado damage track was found with Landsat images.	H
Ivanovo region, Lukh district, 12 km from Lukh city	-	-	-	36310	-	~12:00	No damage to settlements. Tornado damage track was found with Landsat images.	H
Ivanovo region, Yurievets district,	-	-	-	36311	-	~12:40	Dozens of houses in Elmat' village were completely destroyed, some buildings were lifted up and moved for dozen meters, less than 10 people died.	H

17 km from Yurievets city, Elnat village							(Androshin and Bystrova, 1984). The tornado damage track was found with Landsat images.
Nizhniy Novgorod region, Nizhniy Novgorod district, near Shumilovo	-	-	a	1	~11:00 or ~14:00		Tornado- or squall-induced strips of tree damage near Shumilovo (with 50 m width, trees were uprooted or broken at 1–2 m height) (Meteoclub, 2008). No forest disturbances were found with Landsat data.
Kostroma region, Ponazyrevo district, Yakshanga		36308/ 36309/ 36319/ 36320	-	b	1	~13:15	M Two houses in Yakshanga village were uprooted because of tornado (Yakshanga Wiki, 2017). Tornado- or squall-induced forest damage was mentioned (V85a). Amorphous forest disturbances (97 ha) were found with satellite data.
Kirov region, Suna district, Kokui and Suna villages	-	-	-	c	2	15:00–16:00	M Tornado damaged farms and houses in Kokui and Suna villages (houses were uprooted). Trees broken. One broken tree was deeply stuck into the ground (Korobeimikova, 2017). Squall wind gusts up to 30–40 m s ⁻¹ observed in the evening (V85a). No forest disturbances were found with Landsat data.
Yaroslavl region, Liubim district	-	-	-	-	-	~12:30	L Strips of tree damage were mentioned (V85a). No forest disturbances were found with satellite data.
Nizhniy Novgorod region, Nizhniy Novgorod district, near Sormovo	-	-	-	-	-	~11:00 or ~14:00	L Squall-induced strips of tree damage (V85a) near Sormovo. No forest disturbances were found with Landsat data.
Nizhniy Novgorod region, Chkalovsk	-	-	-	-	-	~11:00 or ~14:00	VL Damage to powerlines. 350 houses affected in the entire region (Alimov et al., 1984). Squall wind speed up to 30–40 m s ⁻¹ observed in the evening (V85a). No forest disturbances were found with Landsat data.
Chuvashia republic, Alatyr district	-	-	2	-	-	~14:00	VL Squall wind gusts up to 30–40 m s ⁻¹ observed in the evening (V85a). Alatyr and Kanash regions were the most affected by wind in Chuvashia region. Power lines corrupted, some houses damaged (Alimov et al., 1984). No forest disturbances were found with satellite data.
Chuvashia republic, Kanash district	-	-	2	-	-	~14:00	VL Squall wind gusts up to 30–40 m s ⁻¹ observed in the evening (V85a). Alatyr and Kanash regions were the most affected by wind in Chuvashia region. Power lines corrupted, some houses damaged (Alimov et al., 1984). No forest disturbances were found with Landsat data.
Saratov region, no precise location	-	-	-	-	-	15:00–16:00	VL Squall wind gusts up to 30–40 m s ⁻¹ observed in the evening in Saratov region (V85a). No forest disturbances were found with satellite data.
Moscow and Ryazan regions, no precise location	-	-	-	-	-	~13:00	VL Squall wind gusts up to 30–40 m s ⁻¹ observed in the evening in Moscow and Ryazan regions (V85a). No forest disturbances were found with Landsat data.
Mordovia republic, no precise location	-	-	-	-	-	~14:00	VL Squall wind gusts up to 30–40 m s ⁻¹ observed in the evening in Mordovia republic (V85a). No forest disturbances were found with Landsat data.

Appendix B. Supplementary data

Supplementary data to this article can be found online at <https://doi.org/10.1016/j.atmosres.2018.02.011>.

References

- Alimov, G., Illesh, A., Kozlov, V., Korneyev, V., 1984. 120 minutes of a Tornado. *Izvestia*, June, No 164. (in Russian).
- Androshin, A., Bystrova, Z., 1984. There is No Other's Misfortune. *Pravda*, July, No 190. (in Russian).
- Antonescu, B., Schultz, D.M., Holzer, A., Groenemeijer, P., 2017. Tornadoes in Europe: an underestimated threat. *Bull. Am. Meteorol. Soc.* 98, 713–728.
- Ball, G.H., Hall, D.J., 1965. *ISODATA, a Novel Method of Data Analysis and Pattern Classification*. Stanford Research Institute, Menlo Park.
- Baumann, M., Ozdogan, M., Wolter, P.T., Krylov, A., Vladimirova, N., Radeloff, V.C., 2014. Landsat remote sensing of forest windfall disturbance. *Remote Sens. Environ.* 143, 171–179.
- Berdyshev, V., 2011. Following the Tornado. <https://www.proza.ru/2011/02/09/952>, Accessed date: 14 November 2017 (in Russian).
- Brooks, H.E., 2004. On the relationship of tornado path length and width to intensity. *Weather Forecast.* 19, 310–319.
- Brooks, H.E., 2013. Severe thunderstorms and climate change. *Atmos. Res.* 123, 129–138.
- Chernokulsky, A.V., Kurgansky, M.V., Mokhov, I.I., 2017. Analysis of changes in tornado-genesis conditions over northern Eurasia based on a simple index of atmospheric convective instability. *Doklady Earth Sci.* 477, 1504–1509.
- Cipar, J., Cooley, T., Lockwood, R.B., Grigsby, P., 2004. Distinguishing Between Coniferous and Deciduous Forests Using Hyperspectral Imagery. In: *Proceedings of International Geoscience and Remote Sensing Symposium IGARSS '04*, <http://dx.doi.org/10.1109/IGARSS.2004.1369758>.
- Doswell III, C.A., Burgess, D.W., 1988. On some issues of United States tornado climatology. *Mon. Weather Rev.* 116, 495–501.
- Doswell III, C.A., Evans, J.S., 2003. Proximity sounding analysis for derechos and supercells: An assessment of similarities and differences. *Atmos. Res.* 67–68, 117–133.
- Dyer, R.C., 1988. Remote sensing identification of tornado tracks in Argentina, Brazil, and Paraguay. *Photogramm. Eng. Remote Sens.* 54, 1429–1435.
- Finch, J., Bikos, D., 2012. Russian tornado outbreak of 9 June 1984. *E-J. Sev. Storms Meteorol.* 7, 1–28.
- Forbes, G.S., Wakimoto, R.M., 1983. A concentrated outbreak of tornadoes, downbursts and microbursts, and implications regarding vortex classification. *Mon. Weather Rev.* 111 (1), 220–236.
- Fuhrmann, C.M., Konrad II, C.E., Kovach, M.M., McLeod, J.T., Schmitz, W.G., Dixon, P.G., 2014. Ranking of tornado outbreaks across the United States and their climatological characteristics. *Weather Forecast.* 29, 684–701.
- Fujita, T.T., 1981. Tornadoes and downbursts in the context of generalized planetary scales. *J. Atmos. Sci.* 38, 1511–1534.
- Groenemeijer, P., Kühne, T., 2014. A climatology of tornadoes in Europe: results from the European severe weather database. *Mon. Weather Rev.* 142, 4775–4790.
- Hardisky, M.A., Klemas, V., Smart, R.M., 1983. The influence of soil salinity, growth form, and leaf moisture on the spectral radiance of *Spartina alterniflora* canopies. *Photogramm. Eng. Remote Sens.* 49, 77–83.
- Johns, R.H., Doswell III, C.A., 1992. Severe local storms forecasting. *Wea. Forecasting* 7, 588–612.
- Kapitanova, T.P., 1986. Energetics and kinematics of the cyclone passed 8–10 June 1984 over there European part of the USSR. *Meteorol. Gidrol.* 10, 45–52 (in Russian).
- Korobeinikova, A., 2017. Tamara Caught with the Wind and Began to Blow Away, How the nature raged in Vyatka in the last centuries. Kirov portal. <https://kirov-portal.ru/blog/tamaru-podhvatilo-vetrom-i-stalo-unosit-kak-bushevala-stihiya-na-vyatke-v-proshlyh-stoletiyah-3961-23163/>, Accessed date: 14 November 2017 (in Russian).
- Kurgansky, M.V., Chernokulsky, A.V., Mokhov, I.I., 2013. The tornado over Khanty-Mansiysk: an exception or a symptom? *Russ. Meteorol. Hydrol.* 38, 539–546.
- Lassig, R., Mochalov, S.A., 2000. Frequency and characteristics of severe storms in the Urals and their influence on the development, structure and management of the boreal forests. *For. Ecol. Manag.* 135, 179–194.
- Lyakhov, M.Y., 1986. Tornadoes in the midland belt of Russia. *Sov. Geogr.* 6, 562–570.
- Matsangouras, I.T., Pytharoulis, I., Nastos, P.T., 2014. Numerical modeling and analysis of the effect of complex Greek topography on tornadogenesis. *Nat. Hazards Earth Syst. Sci.* 14, 1905–1919.
- McDonald, J., Mehta, K.C., 2006. A Recommendation for an Enhanced Fujita Scale (EF-Scale). Wind Science and Engineering Research Center. Texas Tech University, Lubbock.
- Meteoclub, 2008. As It Was Then. 29 Jul 2008. <http://meteoclub.ru/index.php?action=vtthread&forum=2&topic=145&page=10#25>, Accessed date: 14 November 2017 (in Russian).
- Molthan, A.L., Bell, J.R., Cole, T.A., Burks, J.E., 2014. Satellite-based identification of tornado damage tracks from the 27 April 2011 severe weather outbreak. *J. Oper. Meteorol.* 2, 191–208.
- Myint, S.W., Yuan, M., Cerveny, R.S., Giri, C., 2008. Comparison of remote sensing image processing techniques to identify tornado damage areas from Landsat TM data. *Sensors* 8, 1128–1156.
- Novitskii, M.A., Pavlyukov, Y.B., Shmerlin, B.Y., Makhnorylova, S.V., Serebryannik, N.I., Petrichenko, S.A., Tereb, L.A., Kalmykova, O.V., 2016. The tornado in Bashkortostan: the potential of analyzing and forecasting tornado-risk conditions. *Russ. Meteorol. Hydrol.* 41, 683–690.
- Okada, R., Katsumura, A., Tamura, Y., Matsui, M., Yoshida, A., 2015. Development of Japanese Enhanced Fujita Scale. In: *Summaries to Technical Papers of Annual Meeting, Japan Association for Wind Engineering*, pp. 125–126.
- Peyraud, L., 2013. Analysis of the 18 July 2005 tornadic supercell over the Lake Geneva region. *Weather Forecast.* 28 (6), 1524–1551.
- Púčik, T., Groenemeijer, P., Rädler, A.T., Tijssen, L., Nikulin, G., Prein, A.F., van Meijgaard, E., Fealy, R., Jacob, D., Teichmann, C., 2017. Future changes in European severe convection environments in a regional climate model ensemble. *J. Clim.* 30, 6771–6794.
- Rozhkov, A.A., Kozak, V.T., 1989. *Forest Sustainability*. Agropromizdat, Moscow (in Russian).
- Sayn-Wittgenstein, L., Wightman, J.M., 1975. Landsat Application in Canadian forestry. In: *Proceeding of the 10th Int Symp on Remote Sensing of Environment*. 2. pp. 1209–1218.
- Sheremetyevo 50th Anniversary, 2009. Tornado of 9 June 1984. 7 April 2009. Livejournal. <http://sheremetyevo-50.livejournal.com/2801.html>, Accessed date: 14 November 2017 (in Russian).
- Shikhov, A., Chernokulsky, A., 2018. A satellite-derived climatology of unreported tornadoes in forested regions of northeast Europe. *Remote Sens. Environ.* 204, 553–567.
- Sklyarenko, V.M., Shcherbak, G.V., Il'chenko, A.P., Ochkorva, O.Yu., Isaenko, O.Ya., 2009. The Hundred Notorious Disasters. Phoenix, Moscow (in Russian).
- Snitkovskiy, A.I., 1987. Tornadoes in the USSR. *Meteorol. Gidrol.* 9, 12–25 (in Russian).
- Solenikov, A., 2006. Sartovo: Life after Tornado. *Severniy Kray*. <http://www.sevkray.ru/news/5/5014>, Accessed date: 14 November 2017 (in Russian).
- Szwagrzyk, J., Gazda, A., Dobrowolska, D., Chečko, E., Zaremba, J., Tomski, A., 2017. Tree mortality after wind disturbance differs among tree species more than among habitat types in a lowland forest in northeastern Poland. *For. Ecol. Manag.* 398, 174–184.
- Taszarek, M., Czernecki, B., Walczakiewicz, S., Mazur, A., Kolendowicz, L., 2016. An isolated tornadic supercell of 14 July 2012 in Poland — a prediction technique within the use of coarse-grid WRF simulation. *Atmos. Res.* 178–179, 367–379.
- Taszarek, M., Brooks, H.E., Czernecki, B., 2017. Sounding-derived parameters associated with convective hazards in Europe. *Mon. Weather Rev.* 145, 1511–1528.
- Tijssen, L., 2015. *Tornado Outbreaks in Europe*. Master Thesis. University of Utrecht, Utrecht.
- Toomey, M., Vierling, L.A., 2005. Multispectral remote sensing of landscape level foliar moisture: techniques and applications for forest ecosystem monitoring. *Can. J. For. Res.* 35, 1087–1097.
- Vasiliev, A.A., Peskov, B.E., Snitkovskiy, A.I., 1985a. Tornadoes on 9th of June 1984. *Gidrometizdat, Leningrad*.
- Vasiliev, A.A., Peskov, B.E., Snitkovskiy, A.I., 1985b. Tornadoes, squalls and hail of 8–9 June 1984. *Sov. Meteorol. Hydrol.* 8, 1–9.
- Vorovencii, I., 2014. Detection of environmental changes due to windthrows using landsat 7 ETM+ satellite images. *Environ. Eng. Manag. J.* 13 (3), 565–576.
- Wang, F., Xu, Y.J., 2010. Comparison of remote sensing change detection techniques for assessing hurricane damage to forests. *Environ. Monit. Assess.* 162, 311–326.
- Wang, W., Qu, J.J., Hao, X., Liu, Y., Stanturf, J.A., 2010. Post-hurricane Forest damage assessment using satellite remote sensing. *Agric. For. Meteorol.* 150, 122–132.
- Wiki, Yakshanga, 2017. 11 July. https://wiki2.org/ru/%D0%AF%D0%BA%D1%88%D0%B0%D0%BD%D0%B3%D0%B0_%D0%BF%D0%BE%D1%81%D1%91%D0%BB%D0%BE%D0%BA, Accessed date: 14 November 2017 (in Russian).
- Yuan, M., Dickens-Micozzi, M., Magsig, M.A., 2002. Analysis of tornado damage tracks from the 3 May tornado outbreak using multispectral satellite imagery. *Weather Forecast.* 17, 382–398.